JOINT INVERSION FOR THREE-DIMENSIONAL VELOCITY STRUCTURE OF THE BROADER AFRICA-EURASIA COLLISION REGION

Megan P. Flanagan[2], Eric M. Matzel[2], Suzan van der Lee[1], Heather Bedle[1], Michael E. Pasyanos[2], Federica Marone[3], Barbara Romanowicz[3], Christian Schmid[4], and Arthur J. Rodgers[2]

Northwestern University[1], Lawrence Livermore National Laboratory[2], UC Berkeley[3], ETH Zurich[4]

Sponsored by National Nuclear Security Administration
Office of Nonproliferation Research and Development
Office of Defense Nuclear Nonproliferation

Contract No. DE-FC52-04NA25541[1], W-7405-ENG-48[2], and DE-FC52-04NA25542[3]

ABSTRACT

We report on progress towards a new, comprehensive three-dimensional model of shear velocity in a broad region extending from the western Mediterranean Sea to the Hindu Kush and encompassing northeastern Africa, the Arabian Peninsula, and the Middle East. Our model will be an integration of regional waveform constraints, surface wave group velocity measurements, teleseismic *P* and *S* arrival times, and crustal thickness estimates. These measurements are made from a combination of MIDSEA, PASSCAL, GeoScope, Geofon, GSN, IDA, MedNet, and local deployments throughout the region. The data offer complementary sensitivity to crust and mantle structures and are jointly inverted to image the complexity of this tectonically diverse area.

We are in the process of assembling each of these data sets and testing the joint inversion for subsets of the data. In this phase of the project we focus on compiling crustal thickness constraints from literature, computing group velocity dispersion measurements, and fitting regional fundamental and higher mode Rayleigh waveforms using the partitioned waveform inversion (PWI) technique. To date we have accumulated over 300 crustal thicknesses from receiver functions, reflection/refraction profiles, and gravity surveys. We have measured Love and Rayleigh wave group velocities for hundreds of new paths recorded at the MIDSEA stations and combined them with thousands of existing paths transecting the region. These new paths have better defined the distribution of anomalies particularly with respect to the boundaries of sedimentary basins at short periods. In addition we have inverted over 3,800 waveforms traversing the Arabian Peninsula, Iran, Afghanistan, the Nubian shield, east African rift zone, and the Russian Platform which extends our original coverage significantly to the east and north.

We also demonstrate the proposed new data-inversion methodology and discuss results from combining these new measurements in a preliminary joint inversion for shear velocity structure. The combined data coverage will ensure that our three-dimensional model comprises the crust, upper mantle, and transition zone with spatially varying, but useful resolution that will allow better calibration of both travel times and waveforms for monitoring throughout the Middle East and North Africa.

OBJECTIVES

Our primary objective is developing a new 3-D S-velocity model for the Middle East and Mediterranean region, including North Africa, southern Europe, and Arabia that

1) is resolved in aseismic regions,
2) is resolved throughout the upper mantle (to 660 km),
3) resolves laterally varying crustal thickness,
4) contains laterally varying vertical velocity gradients,
5) is simultaneously compatible with multiple data sets,
6) utilizes several recent, unique waveform data sets, and
7) includes uncertainties of the model parameters.

These features would increase the model's ability to predict and calibrate regional travel times and waveforms, thereby providing improved event locations, focal mechanisms, and other event discriminants.

Secondly, we aim to convert the 3-D *S*-velocity model to a 3-D *P*-velocity model, using both literature on elastic properties (and their partial derivatives with temperature and pressure) of mantle rocks and empirical information provided by measured arrival times of teleseismic *P* and *P*m*s* waves.

Our third objective is to test both the *S*-and *P*-wave models' ability to predict regional *P* and *S* travel times, deflect wave paths and deform waveforms, and assess their effects first on the studied seismograms (travel times and amplitudes) and subsequently on the 3-D models derived from these data.

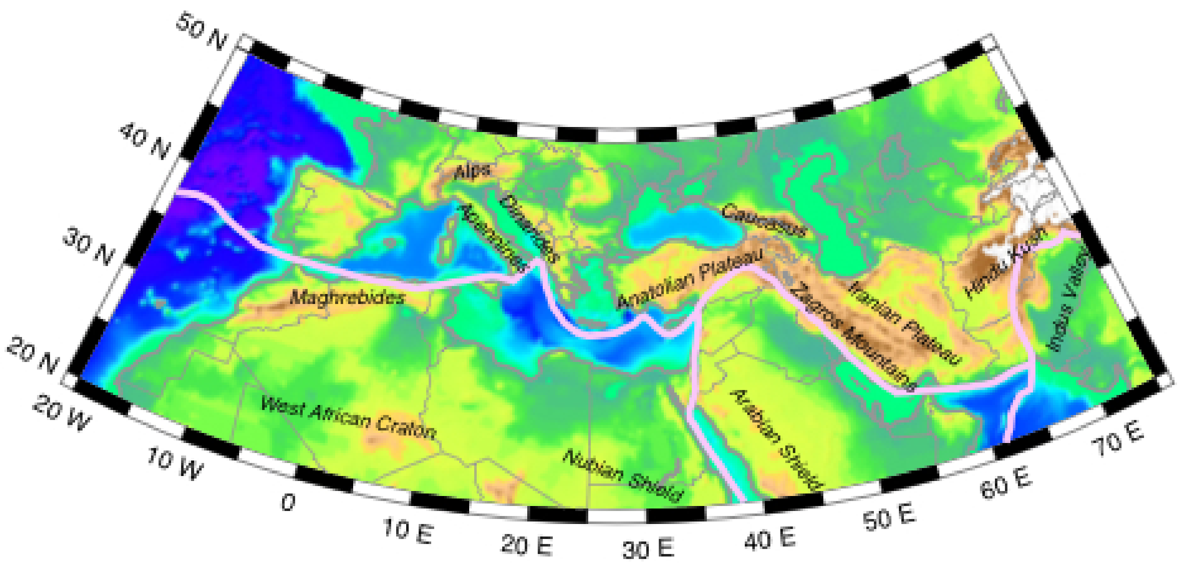

Figure 1. Topographic map of the study region. The pink line is the NUVEL1-A (DeMets et al., 1990) representation of the Eurasia-Africa-Arabia plate boundary.

The study region is centered around the Africa-Arabia-Eurasia triple junction (Figure 1), and extends west to the Africa-Eurasia-North America junction at the Azores, just off the map, and east to the Arabia-Eurasia-Indian Plate junction. The NUVEL1-A (DeMets et al., 1990) representation of these plate boundaries is shown by the pink line in Figure 1. The interaction of these six major tectonic plates with each other and with several microplates within an area ofone quarter of the Earth's circumference yields this region rich with tectonic complexity. The three-dimensional structure of the upper mantle and crust are correspondingly complex. We plan to capture various renditions of this structurally complicated part of the world in one *S*-velocity model through the joint inversion of several different types of seismic data simultaneously; the new model will refine our understanding of the structure and tectonics in this region of the Earth.

RESEARCH ACCOMPLISHED

We have examined over 13,000 available waveforms from the Lawrence Livermore National Laboratory (LLNL) database which sample North Africa and the Middle East and successfully fit about 3800 of them using the non-linear inversion procedure employed by previous partitioned waveform inversion studies (van der Lee and Nolet, 1997: Marone et al. 2004). Six event-station paths for which we have estimated path-average structure are shown in Figure 2 . Earthquakes are indicated by their Harvard Centroid Moment Tensor (CMT) solutions. These six paths sample some of the diversity of geologic/tectonic environments in our study region (Figure 1). The velocity structures were estimated using the average continental model MC35 as a starting model (Van der Lee and Nolet, 1997), however we chose an appropriate crustal thickness for each path (in 5 km increments) based on *a priori* reported estimates. The inversion procedure estimates the perturbations to the starting model by non-linear optimization (Nolet, 1990; van der Lee and Nolet, 1997).

Example Waveform Fits

The waveform fits and resulting shear-velocity profiles for these paths are shown in Figure 3. These models show: 1) faster crustal velocities and slightly faster mantle velocities for the Nubian shield (evid 4074 to AMBATZ); 2) lower velocities in the crust and upper mantle for path crossing the East African Rift (evid 4163 to BGCA); 3) faster crustal and low sub-Moho velocities path from the Gulf of Aden across the Arabian Shield (evid 1325416 to KTLNET); and 4) faster velocities for paths traversing the Russian Platform to the north (evid 6732 to KEV and evid 1323044 to BYKNET).

We attempt to fit both the fundamental and higher mode *S*-waveforms on all three vertical, radial, and transverse components if possible. The following panels show the data (black) and synthetic seismograms for the final model (red). The frequency content of the data and synthetic is different for each fit and generally covers the band 0.006 to 0.1 Hz. The starting model often predicts significant phase differences relative to the data for both the S- and Rayleigh waves. The path across the Nubian Shield (4074-AMBATZ) is faster than the MC35 starting model, and the crustal velocities along this path are quite high. This is consistent with fast crustal velocities in the Arabian Shield (1325416-KTLNET) (e.g., Mokhtar and Al-Saeed, 1994; Sandvol et al., 1998; Rodgers et al., 1999; Julia et al., 2003). It is worth noting that the Red Sea broke up the Nubian-Arabian Shield and these provinces could have similar crustal petrology. Both provinces have volcanics and it has been speculated that mafic intrusion may explain the higher crustal velocities.

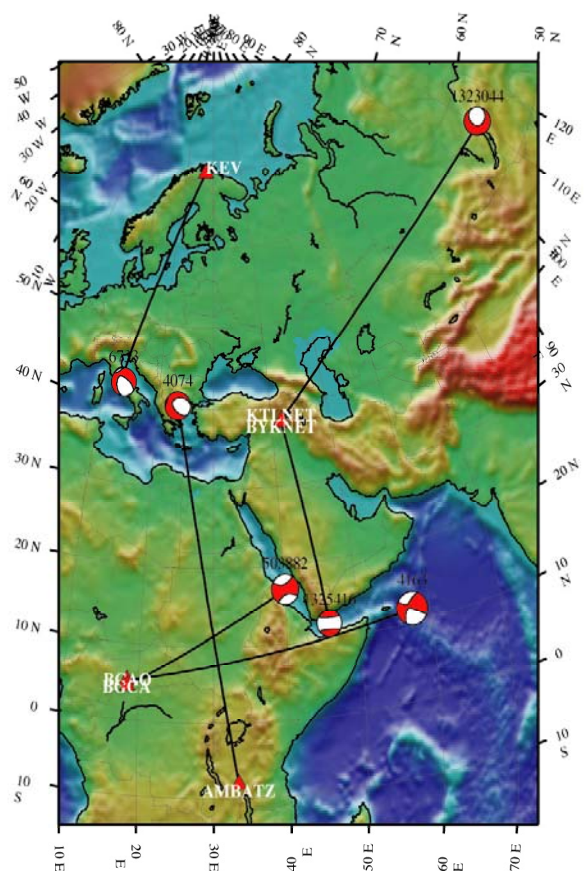

Figure 2. Map of the Western Eurasia and Africa showing six earthquakes and paths for which we fit waveforms. The events are indicated by their moment tensor and identified by their eventid (evid) number. Stations are shown as red triangles.

The inferred mantle velocities beneath the Nubian Shield are slightly faster than the starting model. However, reported mantle velocities beneath the Arabian Shield are lower than average (e.g., Mokhtar and Al-Saeed, 1994; Rodgers et al., 1999, Maggi and Priestley, 2005).

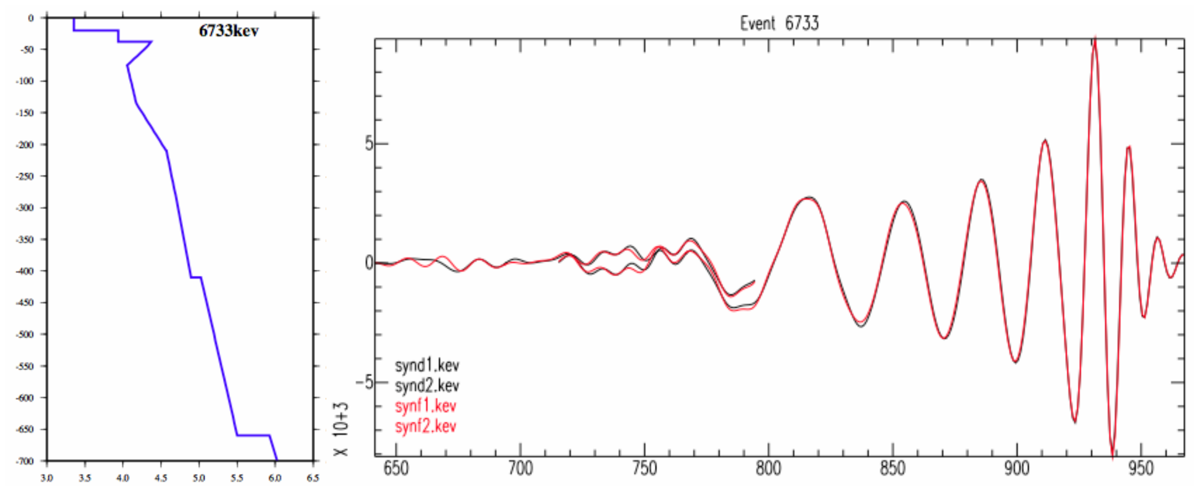

Event 6733 / Station KEV / Transverse component

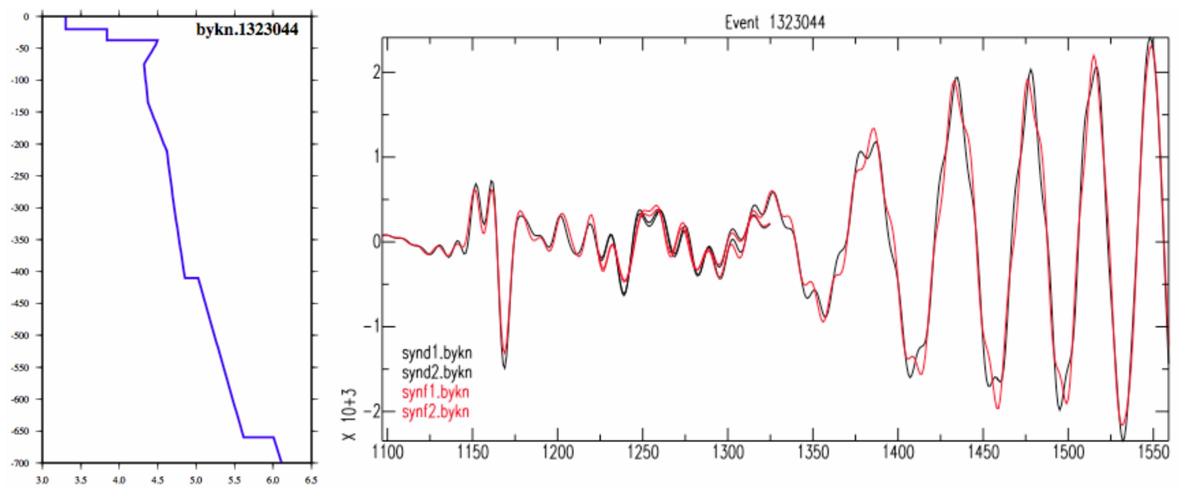

Event 1323044 / Station BYKNET /Transverse component

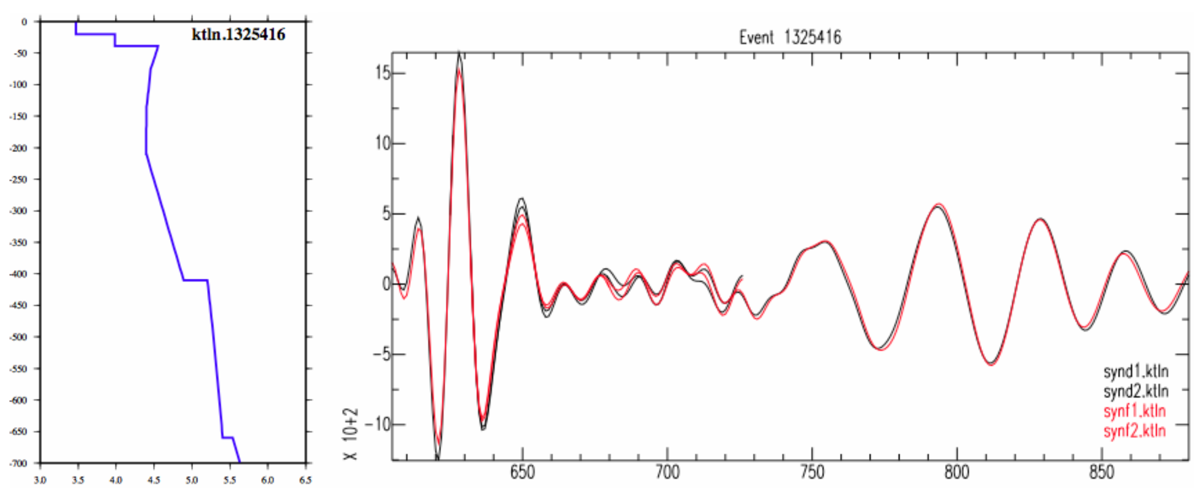

Event 1325416 / Station KTLNET / Radial component

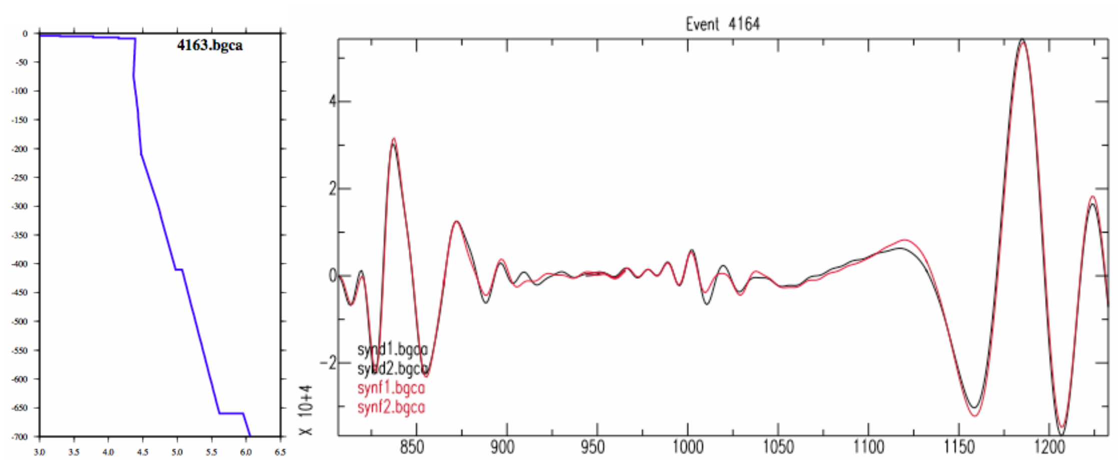

Event 4163 / Station BGCA / Radial component

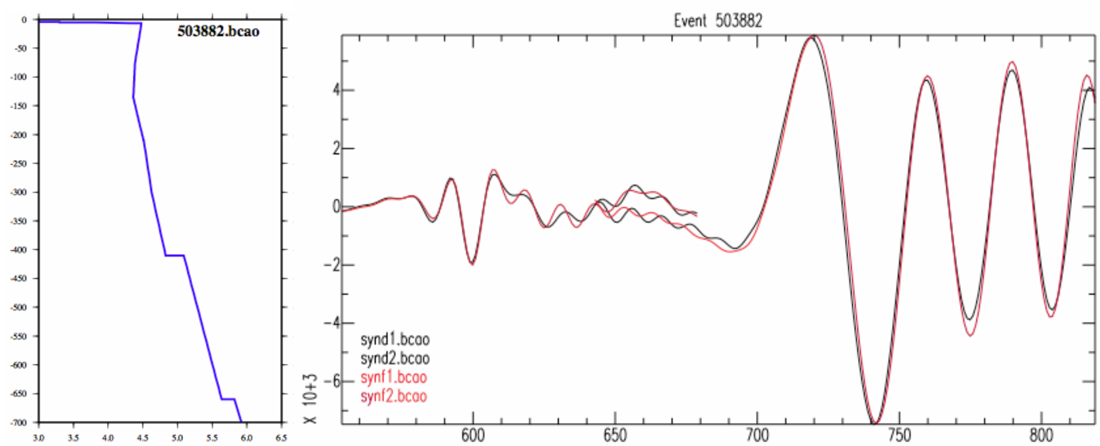

Event 503882 / Station BCAO / Vertical component

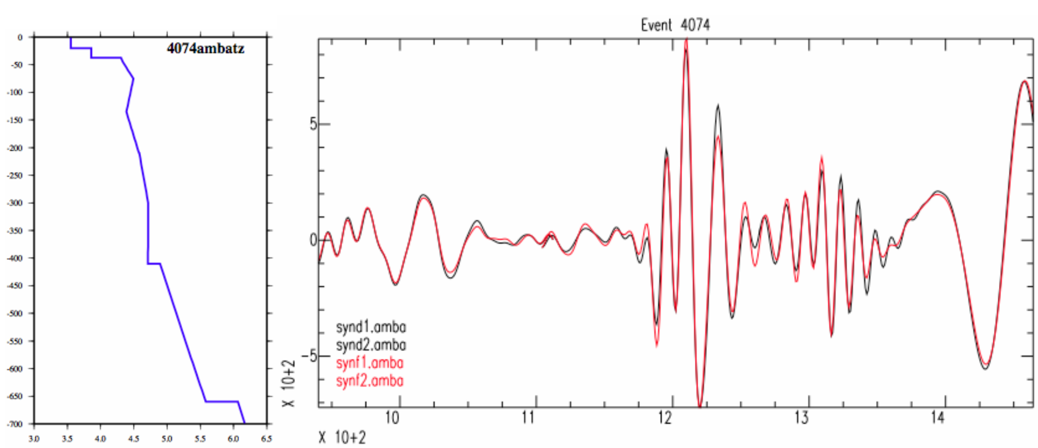

Event 4074 / Station AMBATZ / Vertical component

Figure 3. Example waveform fits (right) and resulting shear velocity profiles (left) for the six paths shown in Figure 2. Data (filtered) is shown in black and the fits in red for three tangential, radial, and vertical components. Note, in some cases the entire wave train is fit (evids 4163 and 4074), and sometimes the body and surface waves are cut and fit separately (evids 6733, 1323044, 1325416, and 503882).

The total ray path coverage is extensive from both the original MIDSEA dataset (Marone et al., 2004) and from data in the LLNL database (shown in Figure 4). We are able to extend the model area significantly to the east and achieve dense sampling of the Arabian Shield, Iran, Afghanistan, and Pakistan. We also have good coverage of northeast Africa, the Red Sea, and parts of the Russian Platform. The 1-D constraints obtained from these ~3,800 waveform fits will be combined with other data sets in the joint inversion for shear velocity structure.

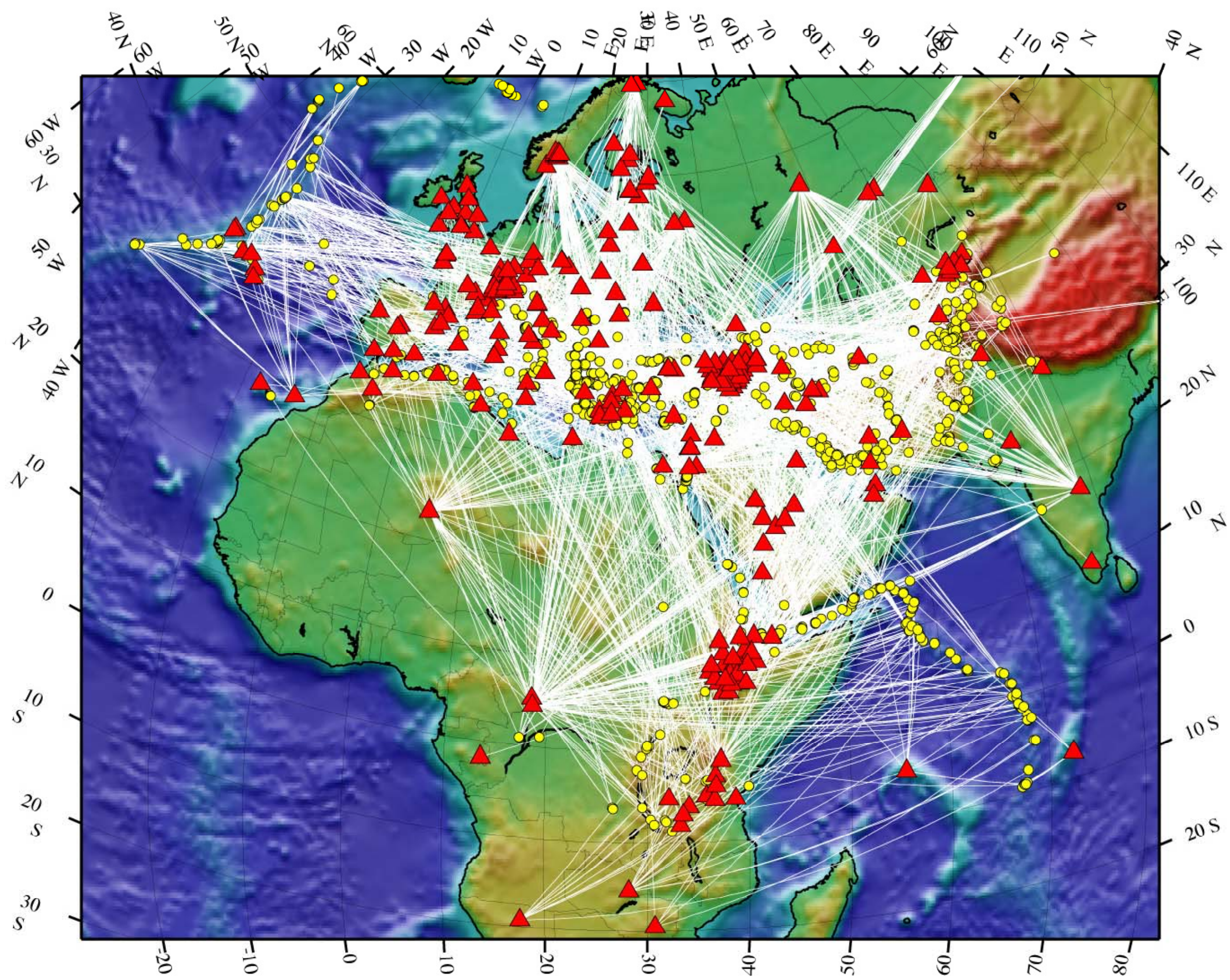

Figure 4. Map of raypath coverage showing all source-receiver paths for the region combining events (yellow circles) with Mb > 5.0 to all recording broadband stations (red triangles) at offsets between 5 and 50 degrees. This represents approximately 3,800 paths from both MIDSEA and LLNL databases.

Surface Wave Group Velocities

We have continued to measure group velocities of Rayleigh waves and use them to update previous group velocity maps (Figure 5). Twenty second Rayleigh waves are very sensitive to crustal structure, which is reflected in the stark group velocity contrast seen in Figure 5 between the oceanic (and Red Sea) regions and the slower continental regions, with thicker crust. Pinpointing the cause of the group velocity differences within continental regions awaits the analysis of the depth distribution of the *S*-velocity anomalies that give rise to the anomalous group velocities. The contrast between the Nubian Shield and Arabian peninsula is, however, qualitatively consistent with the waveform fits and their constraints on upper mantle structure, which show relatively high velocity in the uppermost mantle beneath northeast Africa. This consistency supports the anticipated benefits of a joint inversion as we plan to incorporate the individual group velocity measurements for each path in the joint inversion.

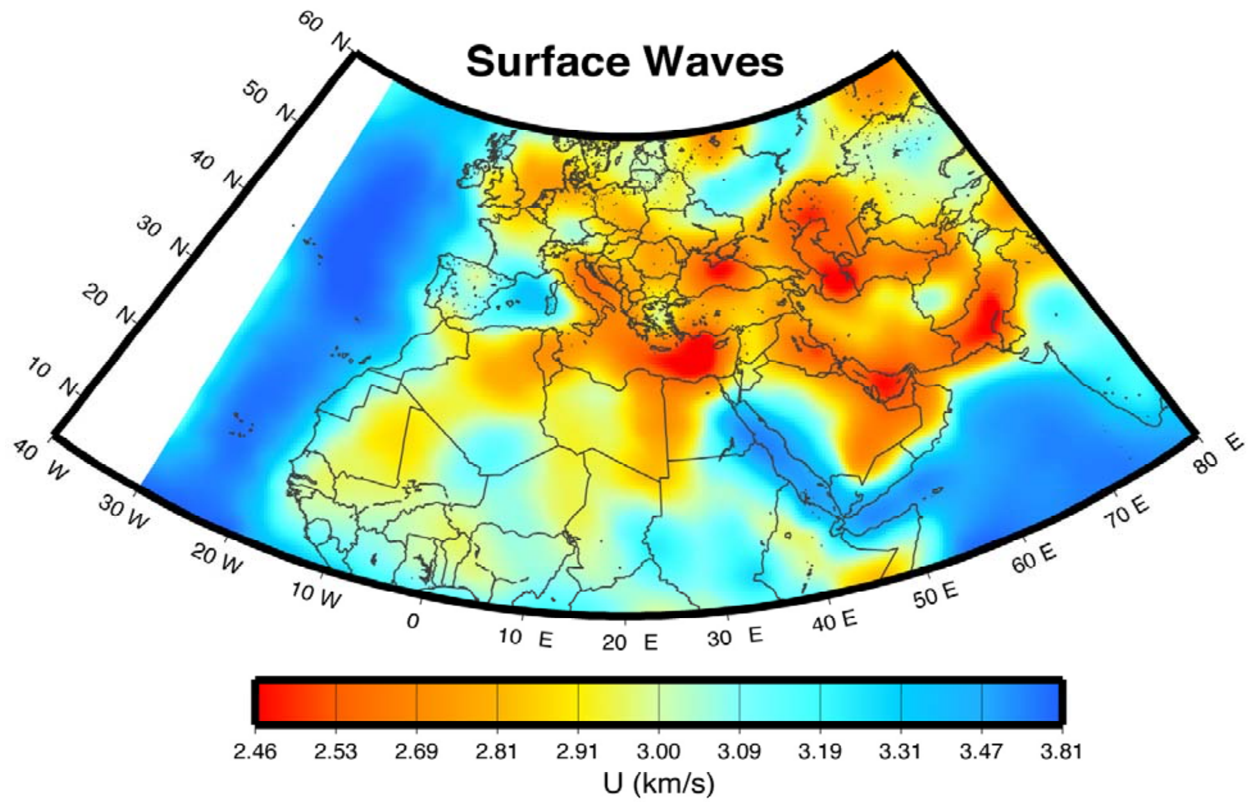

Figure 5. Inferred spatial variation in group velocity (U) for 20 second Rayleigh waves (Pasyanos, 2005).

Crustal Thickness Constraints

We include estimates of crustal thickness as point constraints in the joint inversion and thus compile such measurements from several published studies as shown in Figure 6. We plan to investigate the spatial statistics of these crustal thickness estimates including outlier removal and declustering if necessary before we include them in the joint inversion.

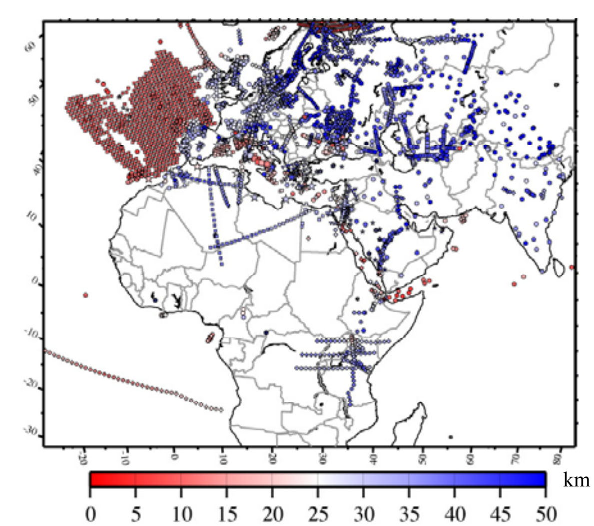

Figure 6. Estimates of crustal thickness including the Mooney et al. (1998) database (circles), receiver function studies (stars), refraction and reflection profiles (squares), and gravity surveys (triangles). The dense points in the Atlantic Ocean are artificially imposed constraints from the MIDSEA study (Marone et al., 2004) due to sparse path coverage from waveform fits.

Teleseismic *S*- and *P*-wave Arrival Times

We plan to include teleseismic *S*- and *P*-wave arrival times and we have collected these data from two different sources thus far (Figure 7).

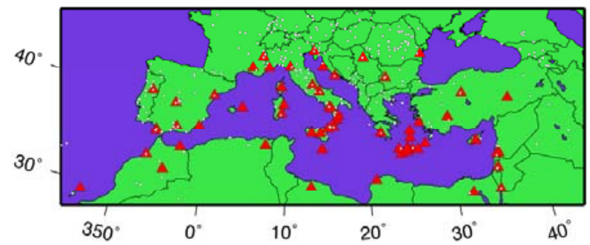

Figure 7. Map of stations used with arrival time data. White circles represent stations for which we extracted absolute delay times from the Engdahl et al. (1998) reprocessed ISC, while red triangles are stations with high-quality relative S-wave delays (between 30 and 90°) obtained using using cross-correlation (Schmid et al., 2006).

Preliminary Inversion Results

To achieve our primary objectives we are developing software that handles the joint inversion of constraints from regional waveform fits, crustal estimates, group velocities, and teleseismic arrival times. We have completed the software for jointly inverting regional waveforms, crustal estimates, and teleseismic arrival times. The joint inversion code has been tested on the teleseismic *S* arrival time data set of Schmid et al. (2006) and the data derived from regional waveform fitting from Marone et al. (2004). The results are encouraging, showing only a percent or two increase in the variance reduction obtained in the linear inversion of both data sets compared to their individual inversions (Schmid et al., 2006). The resolving power of the joint data sets, however, has increased dramatically: the teleseismic data add more lateral resolution to the regional waveform data, while the regional waveform data add more depth resolution to the teleseismic data. The resolved depth range of the combined data sets has doubled with respect to their individual depth ranges. The regional waveform data resolve the upper mantle more strongly while the teleseismic arrival times resolve the lower mantle more strongly. Where the two data sets overlap in spatial sensitivity, (e.g., in the transition zone), the resolving power of the combined data is superior to that of each of the data sets alone.

Upper mantle shear velocity anomalies based on a current inversion of radial and vertical component waveform fits with the crustal constraints is shown in Figure 8. Red regions indicate slower velocities and blue indicate fast. Note the low velocity anomaly beneath the Atlantic Ridge, East Africa Rift, and western Saudi Arabia while fast velocities are seen to the north. These preliminary results are broadly consistent with results from the literature and we do not interpret them further at this point as they are an intermediate step in the whole joint inversion process.

The strength of a joint inversion of different types of seismic data lies in the various data sets being both redundant and complementary. The redundancy is needed to increase accuracy and to ensure that all data sets measure the same structural phenomena. The data sets need to be complementary to increase resolving power over a larger volume of mantle and crust and thereby reduce trade-offs, e.g., between crustal thickness and uppermost mantle velocity, inherent in each type of seismic data set.

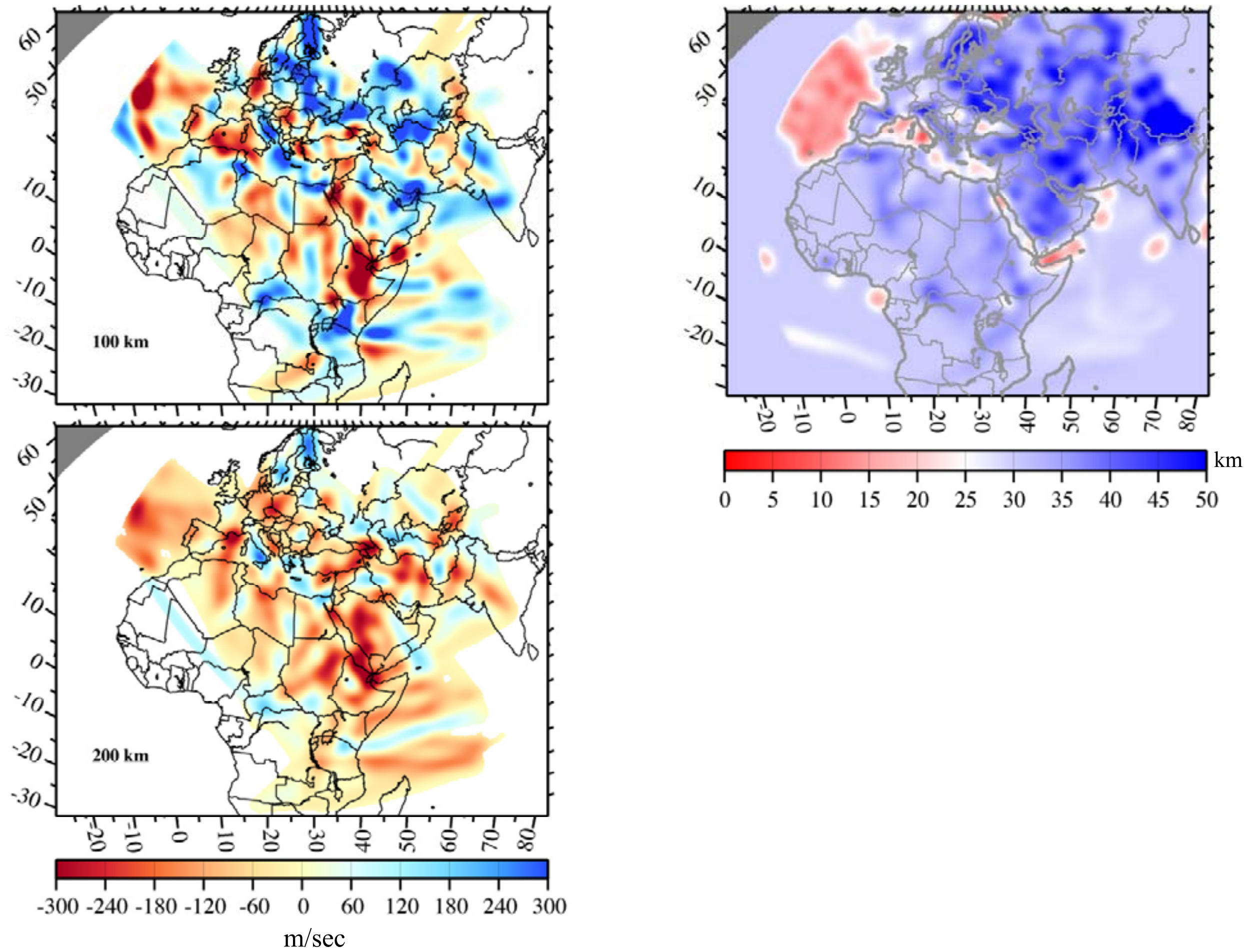

Figure 8. Results from inversion of the regional waveform constraints and crustal thickness estimates. Shear wave velocities at depths of 100 and 200 km are shown to the left where fast (blue) and slow (red) deviations from the starting model are seen. To the right is the resulting map of Moho depth that in some places is driven by the input Moho constraints (from Figure 6). The waveform constraints have been used to interpolate between existing point estimates of crustal thickness in the inversion process to produce this smooth representation.

CONCLUSIONS AND RECOMMENDATIONS

The broad consistency between seismic velocity anomalies inferred from teleseismic arrival times, Rayleigh wave group velocities, and regional waveforms shown here implies that these different types of data sets are at least in part redundant. The consistency further shows that the data sets record the same structural phenomena, despite differences in size and character between typical sensitivity kernels for each data set. This conclusion is further supported by an analysis of how teleseismic delay times depend on frequency (Schmid et al., 2006) and that the teleseismic arrival times and the regional waveforms are highly complementary. The shared sensitivity, though different in character, of receiver functions and Rayleigh wave group velocities to crustal structure is anticipated to separate crustal effects on the observed data from mantle causes when included in the joint inversion.

Preliminary results from data analysis for the Middle East show that this part of the study region is slower on average than typical one-dimensional global velocity models. Marone et al. (2004) and Maggi and Priestley (2005) show that the same is true for the parts of the study region to the west and east, respectively. This allows for a fairly simple set of one-dimensional starting models, yielding a more uniform treatment of data recorded throughout the region.

ACKNOWLEDGEMENTS

Rick Benson of IRIS guided the conversion of the MIDSEA data to SEED format, and Terri Hauk loaded it into the LLNL database.

REFERENCES

DeMets, C. R.G. Gordon, D.F. Argus, and S. Stein (1990), Current plate motions, *Geophys. J. Int*. 101: 425–478.

Engdahl, E.R., van der Hilst, R. and Buland, R. (1998). Global teleseismic earthquake relocation with improved travel times and procedures for depth determination, *Bull. Seis. Soc. Am*. 88: 722–743.

Hatzfeld, D., M. Tartar, K. Priestley and M. Ghafory-Astiany (2003). Seismological constraints on the crustal structure beneath the Zagros Mountain belt (Iran), *Geophys. J. Int.* 155: 403–410.

Julia, J., C. Ammon and R. Herrmann (2003). Lithospheric structure of the Arabian Shield from the joint inversion of receiver functions and surface wave group velocities, *Tectonophysics* 371: 1–21.

Maggi, A. and K. Priestley (2005). Surface waveform tomography of the Turkish-Iranian Plateau, *Geophys. J. Int*. 160: 1068–1080.

Marone, F., S. Van der Lee, and D. Giardini (2004). 3-D upper mantle *S*-velocity model for the Eurasia-Africa plate boundary region, *Geophys. J. Int*. 158: 109–130.

Mokhtar, T. and M. Al-Saeed (1994). Shear wave velocity structures of the Arabian Peninsula, *Tectonophysics* 230: 105–125.

Mooney, W.D., G. Laske, and T.G. Masters (1998). CRUST 5.1: A global crustal model at 5° x 5°, *J. Geophys. Res*. 103: 727–747.

Nolet, G. (1990). Partitioned waveform inversion and 2-dimensional structure under the network of autonomously recording seismographs, *J. Geophys. Res*. 95: 8499–8512.

Pasyanos, M. E. (2005). A varible-resolution surface wave dispersion study of Eurasia, North Africa, and surrounding regions, *J. Geophys. Res*. 110: B12301, doi:10.1029/2005JB003749.

Rodgers, A., W. Walter, R. Mellors, A. M. S. Al-Amri and Y. S. Zhang (1999). Lithospheric structure of the Arabian Shield and Platform from complete regional waveform modeling and surface wave group velocities, *Geophys. J. Int.* 138: 871–878.

Schmid, C., S. van der Lee, J. C. Vandecar, E. R. Engdahl, and D. Giardini (2006). 3-dimensional S-velocity of the mantle in the African-Eurasia plate boundary region from phase arrival times and regional waveforms, *J. Geophys. Res*., in review

Sandvol, E., D. Seber, M. Barazangi, F. Vernon, R. Mellors, and A. Al-Amri (1998). Lithospheric seismic velocity discontinuities beneath the Arabian Shield, *Geophys. Res. Lett*. 25: 2873–2876.

Van der Lee, S., and G. Nolet (1997). Upper-mantle S-velocity structure of North America, J. Geophys. Res., 102:22,815–22,838.

Van der Lee, S., F. Marone, M. van der Meijde, D. Giardini, A. Deschamps, L. Margheriti, P. Burkett, S. C. Soloman, P. M. Alves, M. Chouliaras, A. Eshwehdi, A. Suleiman, H. Gashut, M. Herak, R. Oritz, J. M. Davila, A. Ugalde, J. Vila, and K. Yelles (2001), Eurasia-Africa plate boundary region yields new seismographic data, Eos Trans. AGU, 82: (51), 637–646.